Templated Assembly of Betanin Chromophore on TiO_2: Aggregation-Enhanced Light-Harvesting and Efficient Electron Injection in a Natural Dye-Sensitized Solar Cell

Nicholas A. Treat, Fritz J. Knorr, and Jeanne L. McHale*
Department of Chemistry and Materials Science and Engineering Program
Washington State University, Pullman, WA 99164-4603

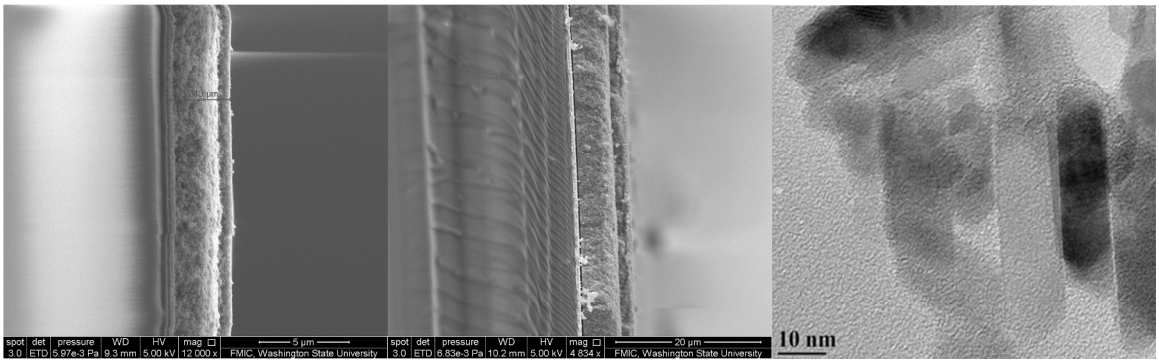

Fig. S1: Scanning electron micrographs of TiO_2 films showing 3.5µm thickness (left), 7µm thickness (middle) and the nanoparticles (right).

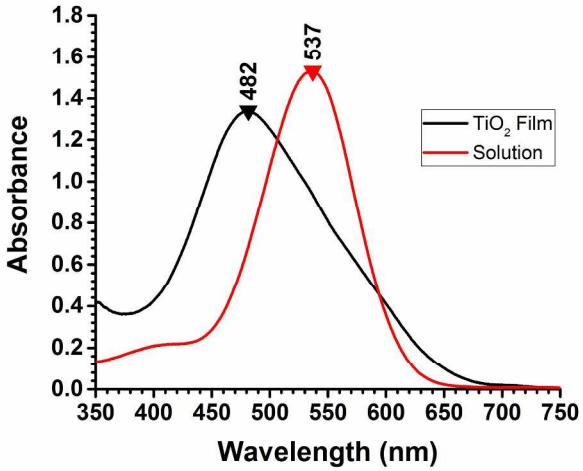

Fig. S2: UV-Vis absorption spectra of the sensitized TiO_2 film (black) and the sensitizing solution (red) showing the dramatic blue-shift from 537nm to 482nm.

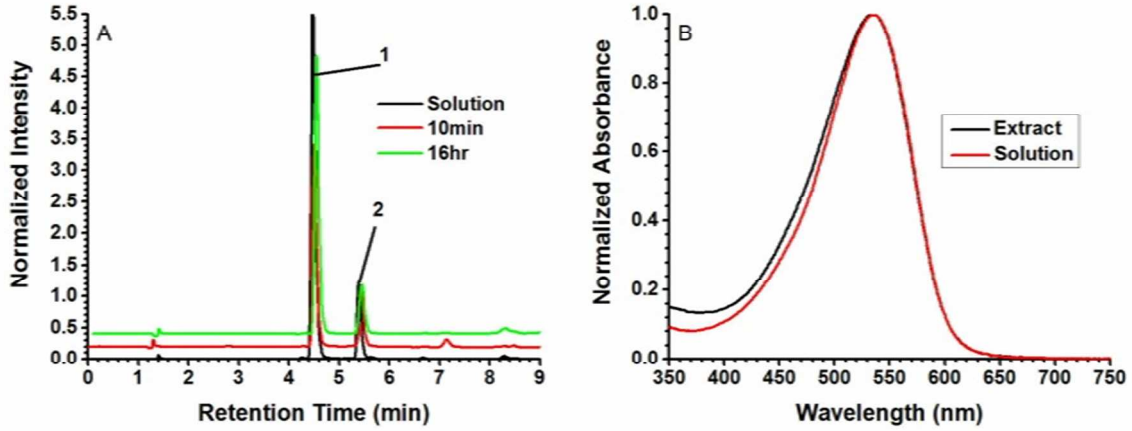

Fig. S3: (A) HPLC chromatogram, monitored at 525nm, of the extracted pigments of films sensitized for 10min (red) and 16hours (green) shown with the sensitizing solution (black) for comparison. Betanin (1) and Isobetanin (2) are the primary components and no significant deviations from the sensitizing solution are observed confirming that betanin degradation does not contribute to the blue-shift observed in the absorption spectra.(B) UV-Vis spectra of the sensitizing solution (Red) and the extract from the film (Black).

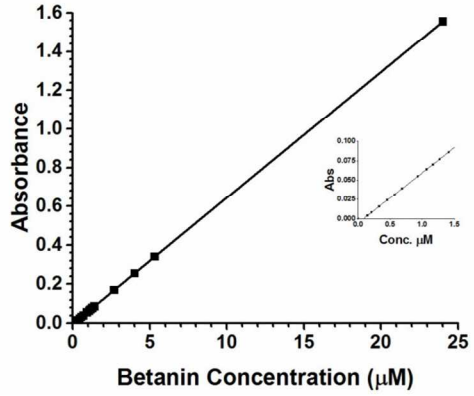

Fig. S4: Calibration curve of betanin vs. calculated concentration. The concentrations of betanin were calculated with the literature value of $\varepsilon = 65{,}000 M^{-1}cm^{-1}$. Despite the use of a literature value, no deviations from linearity were observed over a very wide range of concentrations. Based on our mass measurements of powdered samples, we were able to obtain betanin purified to 50%, $\varepsilon = 31{,}000 M^{-1}cm^{-1}$ by mass with some unknown colorless component. We believe that this component is residual salt and waters of hydration due to the lack of interference with any of our measurements.

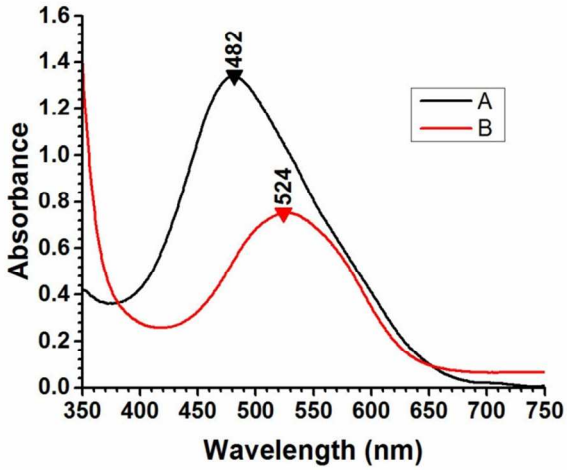

Fig. S5: UV-Vis absorption spectra of films sensitized without l phosphate (A, Black) and with 1mM phosphate (B, red). The peak centers show that the phosphate inhibits the formation of aggregates on the surface since the blue-shift is very minimal, see fig. S1. Based on NMF calculations the addition of 1mM phosphate to the sensitizing solution produced a film with approximately25% aggregate and its components are shown in fig. 3A.

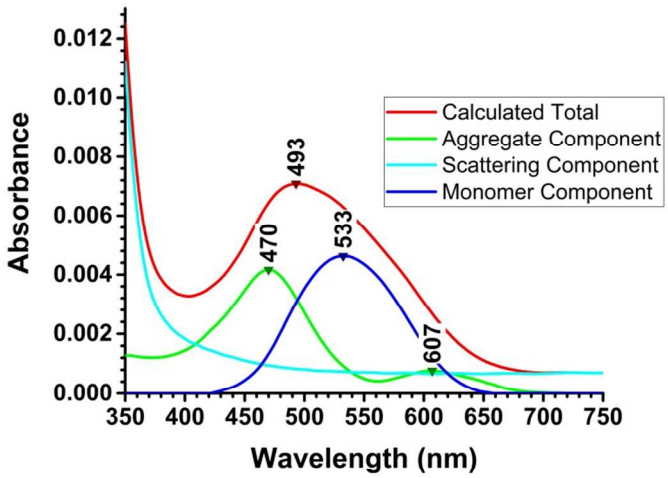

Fig. S6: Unit components from NMF analysis showing the peaks of the aggregate (green), monomer (blue), TiO_2, and the sum of all components (red). Notice that the sum of equal amounts of monomer and aggregate produces an absorbance maximum at 493nm.

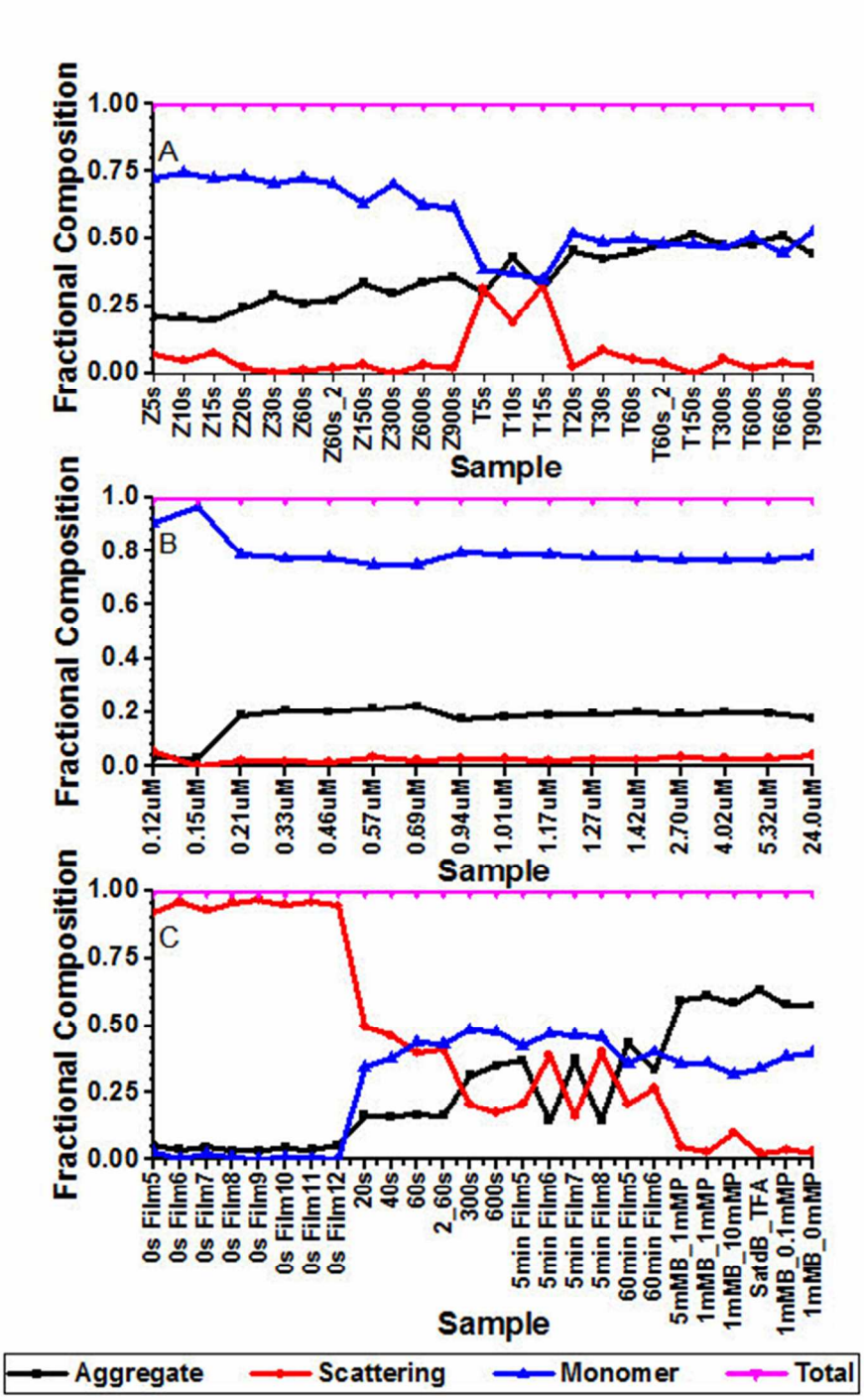

Fig. S7: NMF component analysis showing three subsets of the samples used for: fluorescence measurements (A), Beer's Law analysis of solutions (B), and DSSC characterization (C). Their respective compositions are shown: aggregate (black squares), scattering (red circles), monomer (blue triangles), and the total of all components (pink triangles).

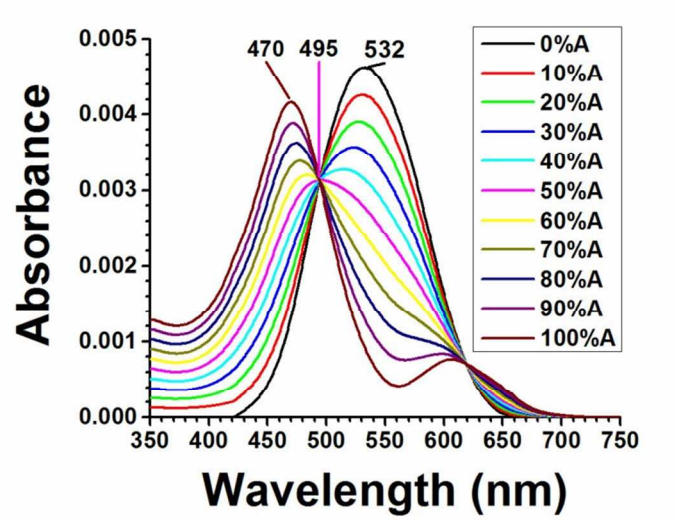

Fig. S8: Linear combination of the aggregate and monomer unit components from the NMF modeling showcasing the representative peak locations for aggregation amounts in 10% intervals. The peak locations from this progression were used to approximate the amount of aggregation on films that were not a part of the original NMF data set. By using this progression, films that displayed flaws in the absorption spectra, from film defects etc., could be analyzed.

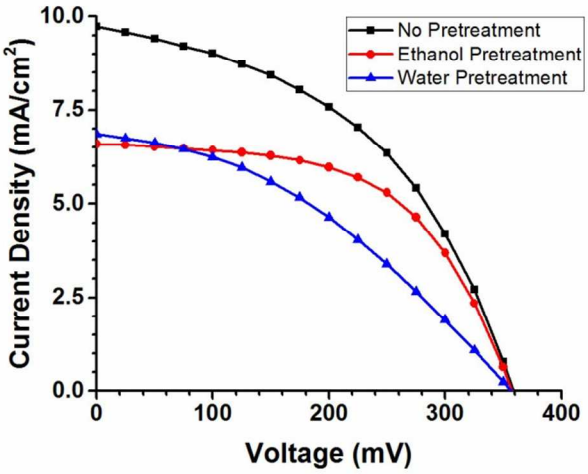

Fig. S9: Characteristic current-voltage plots for films with no pretreatment (black), pretreatment with 0.5M hydrochloric acid in ethanol (red), and purified water (blue). There does not appear to be any correlation between these various pretreatments and the resulting open circuit voltage, which is consistently in the 350-380mV range.